Photoluminescent lateral flow based on non-radiative energy transfer for protein detection in human serum

Alejandro Zamora-Gálvez[a], *Eden Morales-Narváez*[a,b], *Javier Romero*[a], *and Arben Merkoçi*[a,c]*

[a] ICN2 Nanobioelectronics & Biosensors Group, Institut Català de Nanociència i Nanotecnologia, Campus UAB, Bellaterra, Barcelona 08193, Spain.

[b] Biophotonic Nanosensors Laboratory, Centro de Investigaciones en Óptica, A. C. Loma del Bosque 115, Colonia Lomas del Campestre, León 37150, Guanajuato, México.

[c] ICREA Institució Catalana de Recerca i Estudis Avançats, Barcelona 08010, Spain

* arben.merkoci@icn2.cat

Keywords: Lateral flow immunoassay, graphene oxide, quantum dots, fluorescence, protein detection

Abstract

A paper-based lateral flow immunoassay whose photoluminescent properties can be modulated upon protein recognition via the photoluminescence quenching capabilities of graphene oxide (GO) is reported. The assay is intended for the detection of a model protein in human serum, that is, human immunoglobulin G, with the aim to demonstrate a virtually universal protein detection platform. Once the sample is added in the strip, the analyte is selectively captured by antibody-decorated SiO_2 beads (Ab-SiO_2) onto the conjugate pad and the sample flows by capillarity throughout the strip until reaching the test line, where a sandwich-like immunocomplex takes place due to the presence of antibody-functionalized QDs (Ab-QDs) onto the test line. Eventually, GO is added as a revealing agent and the photoluminescence of those sites protected by the complex Ab-SiO_2/Antigen/Ab-QDs will not be quenched, whereas those photoluminescent sites directly exposed are expected to be quenched by GO, including the control line, made of bare QDs, reporting that the assay occurred successfully. Hence, the photoluminescence of the test line is modulated by the formation of sandwich-like immunocomplexes. The proposed device achieves a limit of detection (LOD) of 1.35 ng mL^{-1} in standard buffer, which is lower when compared with conventional lateral flow technology reported by gold nanoparticles, including other amplification strategies. Moreover, the resulting device was proven useful in human serum analysis, achieving a LOD of 6.30 ng mL^{-1} in this complex matrix. This low-cost disposable and easy-to-use device will prove valuable for portable and automated diagnostics

applications, and can be easily transferred to other analytes such as clinically relevant protein biomarkers.

1. **Introduction**

Lateral flow (LF) represents a powerful technique with high relevance in biosensing as it achieves the requirements needed for biosensor devices, including low cost, small amount of the sample, robustness and stability.

Taking into account that in lateral flow strips the samples are driven by capillary forces, lateral flow strips are generally built with four parts, (i) the sample pad in which the sample is added in the strip; (ii) the conjugate pad, where specific antibodies targeting the analyte are conjugated with nanoparticles (most commonly gold nanoparticles); the detection pad that includes two different lines where the main immunoreactions take place, that is to say the control and test line. The test line is typically printed with antibodies targeting the analyte, while the control line is printed with other antibodies that capture the antibody that is tagged with an optically active material and comes from the conjugate pad. (iv) The absorbent pad, which operates as the pump of the system. Thus, after adding the sample, the labeled antibodies of the conjugate pad flow throughout the detection pad until they reach the test line , where a sandwich immunocomplex is performed provided the analyte is present in the sample, giving a signal depending of the analyte concentration. On the other hand, as mentioned above, the antibodies coming from the conjugate pad are always captured onto the control line to report that the analysis has been carried out correctly. Consequently, this technology can perform fast measurements and does not need qualified staff to be manipulated. (Posthuma-Trumpie et al., 2009; Quesada-González and Merkoçi, 2015; Sajid et al., 2015) However, LF has some drawbacks, for example at low concentrations of analyte this technology may present problems in terms of sensitivity. Furthermore, its membrane can saturate at high concentrations of the analyte and false negatives may appear as the membrane can be obstructed by different compounds presents in the analysed matrix and provoke unspecific absorptions. In this work, we strive to further LF technology by tackling the drawback of this technique related to its sensitivity.

There is a high demand for the rapid and low-cost determination of proteins, (Fredriksson et al., 2002; Vollmer et al., 2002) particularly for medical applications. In this context, the most widely used tests are based on colorimetric procedures in which proteins react to produce colorimetric complexes, but nowadays other methods such as fluorimetry, (Xue et al., 2012;

Zhang et al., 2012) chemiluminescence (Roda and Guardigli, 2012) and spectrophotometry (Boja and Rodriguez, 2012) are being implemented for protein detection. These techniques represent an improvement in terms of sensitivity and selectivity in comparison with classical methods, such as colorimetric assays. In particular, we focus on photoluminescence measurements for the detection of a model protein, that is human immunoglobulin G. Photoluminescence has great advantages, (Wang and Ni, 2014; Yi et al., 2013) including a great sensitivity and excellent specificity, given that the devices intended for photoluminescence measurement are highly specific and less susceptible to interferences as few materials can absorb and emit light. Furthermore, this technique is simply to perform and is fast to measure.

Our research team possesses experience in the usage of photoluminescent techniques and lateral technology flow-based devices.(Gravagnuolo et al., 2015; Zor et al., 2015) In a previous work, our team reported a photoluminescent LF for the detection of *Escherichia coli* (*E. coli*) using graphene oxide (GO) as a pathogen-revaling agent (Morales-Narváez et al., 2015). In that work, *E coli* was employed as a spacer avoiding non-radiative energy transfer between photoexcited quantum dots (decorated with anti-E. coli antibodies and printed on the test line) and GO, which is known to be an excellent quencher of quantum dots.(Morales-Narváez et al., 2012) Importantly, using graphene related materials, non-radiative energy transfer is observable up to ~30 nm.(Gaudreau et al., 2013) In this regard, bacteria is an excellent spacer facilitating the successful operation of the previously reported LF,(Morales-Narváez et al., 2013) whereas this LF configuration is not applicable to protein detection since proteins are nanoscaled analytes (around 10 nm). Hence, in this research we engineered a new LF configuration and sought to achieve a highly sensitive photoluminescent lateral flow device for protein detection.

The proposed biosensor consist in a paper-based strip, this approach combines anti-human immunoglobulin G (IgG) antibodies with quantum dots nanocrystals (CdSe@ZnS) as a highly specific photoluminescence probe (Ab-QDs) onto the test line and bare QDs printed onto the control line. Aiming at designing an integrated device, we also employ SiO_2 beads functionalized with anti-human IgG antibodies (Ab-SiO_2) in the respective conjugated pad. Importantly, these SiO_2 beads are able to operate as a powerful spacer between photoexcited QDs and GO, avoiding non-radiative energy transfer as their diameter is greater than the nanoscale (300 – 600 nm). Once the sample is added in the strip, the analyte is selectively

captured by the Ab-SiO_2 beads onto the conjugate pad and the sample flows by capillarity throughout the strip until reaching the test line, where a sandwich-like immunocomplex takes place due to the presence of Ab-QDs onto the test line. Eventually, GO is added as a revealing agent and the photoluminescence of those sites protected by the complex Ab-SiO_2/Antigen/Ab-QDs will not be quenched, whereas those photoluminescent sites directly exposed are expected to be quenched by GO, including the control line reporting that the assay occurred successfully. Hence, the photoluminescence of the test line is modulated by the formation of sandwich-like immunocomplexes (see Figure 1).

2. Results and discussion

As the assay depends on photoluminescent signals, we firstly optimized the concentration of the involved QDs. To this end, a strong photoluminescent signal hindering saturation of the LF reader should be chosen, whereas weak photoluminescent signals should be avoided. Consequently, as depicted in Figure S1, we printed different QD concentrations (from 4 to 11 nM) onto various strips and measured their intensities utilizing a lateral flow reader (excitation wavelength of 365 nm, emission filter centered at 670 nm). Through these experiments we determined that 8 nM was an optimal concentration of this reagent as it displays a strong intensity of up to 75% of the dynamic range of the LF reader, thus avoiding saturation.

We then explored different concentrations of GO so as to reach the maximum quenching of QDs in terms of the ratio initial intensity (before GO) / final intensity (after GO). To this end, different water-based suspensions of GO were directly added in the sample pad of several strips printed with QDs concentrated at 8 nM. Among several concentrations of GO, ranging from 70 to 120 µg mL^{-1}, a GO concentration of 90 µg mL^{-1} was picked to yield a maximum quenching efficiency around 85% in both lines, test and control line, avoiding saturation of the flow due to a saturation of GO in the strip as it occurs with higher GO concentrations (see Figure S2). It is worth mentioning that according to the manufacturer's characterization, the GO monolayer we are employing has an average lateral size of 500 nm and a carbon / oxygen ratio around 1.

In order to optimize the spacer agent avoiding highly efficient non-radiative energy transfer, we also investigated two sizes of SiO_2 beads utilized as spacers between photoexcited QDs and GO, including monodispersed beads of 300 and 650 nm respectively (see Figure S3). To this end, SiO_2 beads were previously conjugated to anti human IgG antibodies and embedded into the conjugation pad as described in the experimental section. We carried out our LF

approach using a standard buffer as a matrix, from now and the termed as immunobuffer, that is a mixture of phosphate-buffered saline 0.01M, bovine serum albumin 1% w/v, and Tween 20 0.5%, and different concentrations of the analyte, ranging from 65 to 1000 ng mL^{-1}. Blank samples were also analyzed. Figure S4 shows the overall sensitivity achieved by these assays, showing that the usage of SiO_2 beads of 650 nm facilitates a better sensitivity in the assay probably due to its better efficiency as a bigger spacer that simultaneously amplifies the protected area that will not be quenched by GO.

Figure S5 shows the relationship between the analyte concentration and the quenching effect in the proposed LF approach, where the highest concentrations of the analyte trigger the strongest photoluminescent signals, as quenching is avoided due to the operational principle of this biosensing approach. Hence, the quenching of the test line; Q_{TL}, defined as the final intensity of the test line divided by the initial intensity of the test line, has maximum values around 0.8 units, whereas the quenching of the control line; Q_{CL}, similarly defined as Q_{TL}, remains constant with values of less than 0.2 units. On the contrary, the lowest concentrations of the analyte give rise to highly efficient non-radiative energy transfer since SiO_2 beads are scarcely present and thus GO is able to interact directly with the photoluminescent probes, mainly by physical adsorption forces, pi-pi stacking interactions and hydrogen bonding forces that can occur between GO and biomolecules such as proteins (Morales-Narváez et al., 2013). Consequently, the Q_{TL} values tend to approximate to those values of the Q_{CL} (see Figure 3A)
In order to confirm the operational principle of the proposed LF strip, we investigated its different components via scanning electron microscopy (SEM). The SEM micrographs in Figure 2 reveal how SiO_2 beads are efficiently anchored onto the test line (Figure 2A) and absent onto the control line (Figure 2B) due to the highly specific aforementioned immunoreaction. Panels B and D in Figure 2 display GO-coated LF strips, confirming that GO is able to flow throughout the strip and interact with the control and test line.

Figure 3B displays a normalization in terms of the Q_{TL}/Q_{CL} ratio and the limit of detection (LOD) was calculated using this ratio in the analyzed blank sample plus 3 times its standard deviation. The LOD was determined to be c.a. 3.64 ng mL^{-1} (Figure S6A). At this point, this LF approach starts becoming advantageous in terms of LOD when compared with other LF approaches targeting IgG as it can be observed in Table 1. However, we sought to improve the LOD of the LF approach even further. To this end, we replaced the capture polyclonal

antibody of the test line by a monoclonal antibody. It is well- known that monoclonal antibodies are able to improve both, sensitivity and specificity in immunoassays.(Deguchi et al., 2009) Hence, we tested this new configuration following the methods detailed in the experimental section and found that the usage of such a monoclonal antibody benefited the LOD of the LF approach. Figure 3C-D depicts the overall biosensing performance of this new configuration exhibiting a LOD of c.a. 1.35 ng mL^{-1}, obtaining a significant improvement in the system sensitivity compared with the conventional methods. Figure S6B displays the corresponding calibration curve.

Moreover, in order to prove that this approach can be applied in real sample analyses, the resulting LF strip was also employed in human serum analysis. We employed human immunoglobulin (IgG/IgM/IgE)-depleted serum as a complex matrix that we spiked with different concentrations of IgG, ranging from 1000 ng mL^{-1} until 16 ng mL^{-1}. Blank samples of this matrix were also analyzed. The prepared solutions can be directly added in the strip, though a washing step is necessary in order to remove possible interferences contained in such a complex matrix. This washing process was performed by adding 100 µL of immunobuffer once the sample is dried in the strip. After performing a calibration curve, the limit of detection this approach in human serum was 6.30 ng mL^{-1}, calculated using the aforementioned definition of LOD. It is obvious that the matrix effect affects the overall analytical performance; however, this effect is well known in immunoassays, (Morales-Narváez et al., 2014) and these experiments demonstrate the high sensitivity and selectivity of the proposed lateral flow approach even in a complex matrix.

3. Conclusion

A novel design based on lateral flow technology in combination with quantum dots and the usage of graphene oxide as revealing agent for specific, selective and highly sensitive protein detection has been explored. The overall analytical performance of the system was successfully explored in different matrices, including standard buffer and human serum, showing an advantageous limit of detection of 1.35 ng mL^{-1} and 6.30 ng mL^{-1}, respectively. In comparison with other lateral flow immunoassays targeting human IgG, the developed biosensor presents excellent results in terms of LOD and its adequate behavior in human serum analysis proves that it can be a valuable tool in real sample analysis.

Besides, LFA is a versatile and easy adaptable technique. Each component of the system can be easily modified with the aim of adapting the assay to a different target, obtaining the

possibility of a multidetection platform. The good point of paper-based diagnostics is that there are suitable for large scale production, making them a very cheap and efficient technology. This result could open the way to the use this LF in more diagnostics applications, especially in a medical or laboratory context, due to the lower limit of quantification obtained and improvement of the actual techniques for immunoglobulins detection with lateral flow.

4. Experimental Section

4.1 Reagents and materials

Streptavidin-Quantum dots 655 were purchased from Life Technologies (Eugene, OR, USA). Anti human IgG (whole molecule, I1886), Human immunoglobulin depleted serum was purchased from Celprogen (Torrance,CA, USA) , IgG (I4506), PBS tablets and Tween 20 were purchased from Sigma Aldrich (Madrid, Spain). Polyclonal antihuman IgG antibody conjugated with biotin (ab6869) and monoclonal Antihuman IgG antibody (ab99759) was pu0rchased form Abcam (Cambridge, UK). SiO_2 beads were purchased from Microparticles GmbH (Berlin, Germany). Graphene oxide was purchased from Angstron Materials (Dayton, OH, USA), bovine serum albumin, laminated cards (HF000MC100), nitrocellulose membranes (SHF1800425), sample and adsorbent pads (CFSP001700) were purchased from Millipore (Billerica, MA, USA).

An ESEQuant lateral flow reader from Qiagen GmbH (Stockach, Germany) was used to perform measurements on the LF strips. Biospot Bt-500 reagent dispersing system from Biofluidix (Freiburg, Germany). TS-100 thermoshaker from Biosan (Riga, Latvia) was utilized to perform the conjugation of QDs with antibodies. JP Selecta 2000210 oven from JP selecta (Barcelona, Spain) was used to dry lateral flow strips. SEM analysis was performed using FEI Magellan (Hillsboro, Oregon, USA).

2.1. Lateral flow strip preparation

Conjugation of QDs with antibodies. Biotinylated antibodies were easily conjugated with streptavidin-QDs. Streptavidin-QDs and biotinylated anti-IgG, were mixed at final concentrations of 8nM (QDs) and 300 µg mL^{-1} (anti-IgG), respectively, using a thermosshaker set at 600 rpm and 4 °C for two hours. This conjugation was carried out in immunobuffer (that is, PBS + 1% BSA + Tween 20 0.5%).

The conjugate pad was impregnated with antibody-decorated SiO_2 beads with anti-IgG. Firstly, the conjugate is created by applying successive washing steps in a suspension the SiO_2 beads. To do that, 75 µL of the stock suspension of the beads was added in 925 µL of PBS

buffer. The suspension was then shaken at 650 rpm during 10 minutes and centrifuged at 5000 rpm for 1min in order to precipitate the particles, and facilitate the subsequent removal of the supernatant. To complete the particle washing, the process is repeated three times using PBS, once using PBS supplemented with Tween 20 at 0.05% (PBST) and once with Immunobuffer. Next, 1 mL of anti-human IgG concentrated at 500 µg mL^{-1} in Immunobuffer is added in the pellet of the previously washed particles and this suspension was shaken at 600 rpm for 2h at 4ºC. After this process is finished, a glass fiber strip was soaked by drop casting with the Ab-SiO_2 beads conjugate suspension, and dried at room temperature overnight.

The fabrication of the strips is divided in three parts, (i) assemblage of the detection pad onto the laminated card and and printing of the test and control line onto the detection pad using the Isoflow reagent dispensing system. Antibody-decorated QDs are printed onto the test line, while bare QDs are printed onto the control line and these laminated cards are stored overnight in the fridge (at 8 °C). (ii) Blocking of the detection pad by adding 5 mL of immunobuffer in the laminated card and storing the strip for 15 min in the fridge. Next, the strip is dried in an oven at 37ºC for 90 min. (iii) Sample and absorbent pads are washed and assembled onto the laminated card. This washing procedure involves a washing procedure through ultrapure water, PBST and immunobuffer and a drying process overnight at room temperature. After that the sample and absorbent pads can be assembled onto the laminated card along with the conjugate pad. We normally manufacture strips that are 6 mm with size.

2.2. Overall measurement procedure

Human IgG protein was analyzed at different concentrations ranging from 65 ng mL^{-1} to 1 µg mL^{-1} in immunobuffer. The starting intensity of the lateral flow strip was determined using the ESEQuant lateral flow reader. After adding 100 µL of the sample onto the sample pad, 15 minutes are given for the sample to flow throughout the strip and arrive in the absorbent pad, which is the last part of strip. Next, the strip is dried using an oven at 37ºC for 1 hour, and 100 µL of an aqueous dispersion of GO concentrated at 90 µg mL^{-1} (see Figure S) was added in the sample pad as a revealing agent using the same aforementioned drying procedure (37 ºC for 1 hour). Eventually, the strips are measured using the lateral flow reader. The assays implying human serum analysis may require a washing step before GO addition. To this end, 100 µL of immunobuffer were added in the sample pad in order to eliminate impurities and minimize the matrix effect.

Supporting Information

Supporting Information is available from the Wiley Online Library or from the author.

Acknowledgements

The Nanobiosensors and Bioelectronics Group acknowledges the support from the Generalitat de Catalunya (Grant 2014 SGR 260). ICN2 acknowledges support from the Severo Ochoa Program (MINECO, Grant SEV-2013-0295).

References

1. Boja, E.S., Rodriguez, H., 2012. Mass spectrometry-based targeted quantitative proteomics: Achieving sensitive and reproducible detection of proteins. Proteomics 12, 1093–1110. doi:10.1002/pmic.201100387
2. Deguchi, R., Matsushima, M., Suzuki, T., Mine, T., Fukuda, R., Nishina, M., Ozawa, H., Takagi, A., 2009. Comparison of a monoclonal with a polyclonal antibody-based enzyme immunoassay stool test in diagnosing Helicobacter pylori infection after eradication therapy. J. Gastroenterol. 44, 713–716. doi:10.1007/s00535-009-0069-z
3. Fredriksson, S., Gullberg, M., Jarvius, J., Olsson, C., Pietras, K., Gústafsdóttir, S.M., Östman, A., Landegren, U., 2002. Protein detection using proximity-dependent DNA ligation assays. Nat. Biotechnol. 20, 473–477. doi:10.1038/nbt0502-473
4. Gaudreau, L., Tielrooij, K.J., Prawiroatmodjo, G.E.D.K., Osmond, J., de Abajo, F.J.G., Koppens, F.H.L., 2013. Universal Distance-Scaling of Nonradiative Energy Transfer to Graphene. Nano Lett. 13, 2030–2035. doi:10.1021/nl400176b
5. Gravagnuolo, A.M., Morales-Narváez, E., Matos, C.R.S., Longobardi, S., Giardina, P., Merkoçi, A., 2015. On-the-Spot Immobilization of Quantum Dots, Graphene Oxide, and Proteins via Hydrophobins. Adv. Funct. Mater. 25, 6084–6092. doi:10.1002/adfm.201502837
6. Morales-Narváez, E., Naghdi, T., Zor, E., Merkoçi, A., 2015. Photoluminescent Lateral-Flow Immunoassay Revealed by Graphene Oxide: Highly Sensitive Paper-Based Pathogen Detection. Anal. Chem. 87, 8573–8577. doi:10.1021/acs.analchem.5b02383
7. Morales-Narváez, E., Guix, M., Medina-Sánchez, M., Mayorga-Martinez, C.C., Merkoçi, A., 2014. Micromotor Enhanced Microarray Technology for Protein Detection. Small 10, 2542–2548. doi:10.1002/smll.201303068
8. Morales-Narváez, E., Hassan, A.-R., Merkoçi, A., 2013. Graphene Oxide as a Pathogen-Revealing Agent: Sensing with a Digital-Like Response. Angew. Chemie Int. Ed. 52, 13779–13783. doi:10.1002/anie.201307740
9. Morales-Narváez, E., Pérez-López, B., Pires, L.B., Merkoçi, A., 2012. Simple Förster resonance energy transfer evidence for the ultrahigh quantum dot quenching efficiency by graphene oxide compared to other carbon structures. Carbon N. Y. 50, 2987–2993. doi:http://dx.doi.org/10.1016/j.carbon.2012.02.081
10. Posthuma-Trumpie, G.A., Korf, J., Van Amerongen, A., 2009. Lateral flow (immuno)assay: Its strengths, weaknesses, opportunities and threats. A literature survey. Anal. Bioanal. Chem. 393, 569–582. doi:10.1007/s00216-008-2287-2
11. Quesada-González, D., Merkoçi, A., 2015. Nanoparticle-based lateral flow biosensors. Biosens. Bioelectron. 73, 47–63. doi:10.1016/j.bios.2015.05.050
12. Roda, A., Guardigli, M., 2012. Analytical chemiluminescence and bioluminescence: latest achievements and new horizons. Anal. Bioanal. Chem. 402, 69–76. doi:10.1007/s00216-011-5455-8

13. Sajid, M., Kawde, A.N., Daud, M., 2015. Designs, formats and applications of lateral flow assay: A literature review. J. Saudi Chem. Soc. 19, 689–705. doi:10.1016/j.jscs.2014.09.001
14. Vollmer, F., Braun, D., Libchaber, A., Khoshsima, M., Teraoka, I., Arnold, S., 2002. Protein detection by optical shift of a resonant microcavity. Appl. Phys. Lett. 80, 4057–4059. doi:10.1063/1.1482797
15. Wang, Y., Ni, Y., 2014. Molybdenum Disulfide Quantum Dots as a Photoluminescence Sensing Platform for 2,4,6-Trinitrophenol Detection. Anal. Chem. 86, 7463–7470. doi:10.1021/ac5012014
16. Xue, L., Zhou, X., Xing, D., 2012. Sensitive and Homogeneous Protein Detection Based on Target-Triggered Aptamer Hairpin Switch and Nicking Enzyme Assisted Fluorescence Signal Amplification. Anal. Chem. 84, 3507–3513. doi:10.1021/ac2026783
17. Yi, Y., Deng, J., Zhang, Y., Li, H., Yao, S., 2013. Label-free Si quantum dots as photoluminescence probes for glucose detection. Chem. Commun. 49, 612–614. doi:10.1039/C2CC36282A
18. Zhang, Z., Sharon, E., Freeman, R., Liu, X., Willner, I., 2012. Fluorescence Detection of DNA, Adenosine-5′-Triphosphate (ATP), and Telomerase Activity by Zinc(II)-Protoporphyrin IX/G-Quadruplex Labels. Anal. Chem. 84, 4789–4797. doi:10.1021/ac300348v
19. Zor, E., Morales-Narváez, E., Zamora-Gálvez, A., Bingol, H., Ersoz, M., Merkoçi, A., 2015. Graphene quantum dots-based photoluminescent sensor: A multifunctional composite for pesticide detection. ACS Appl. Mater. Interfaces 7, 20272–20279. doi:10.1021/acsami.5b05838

Figure 1. Scheme of the developed lateral flow

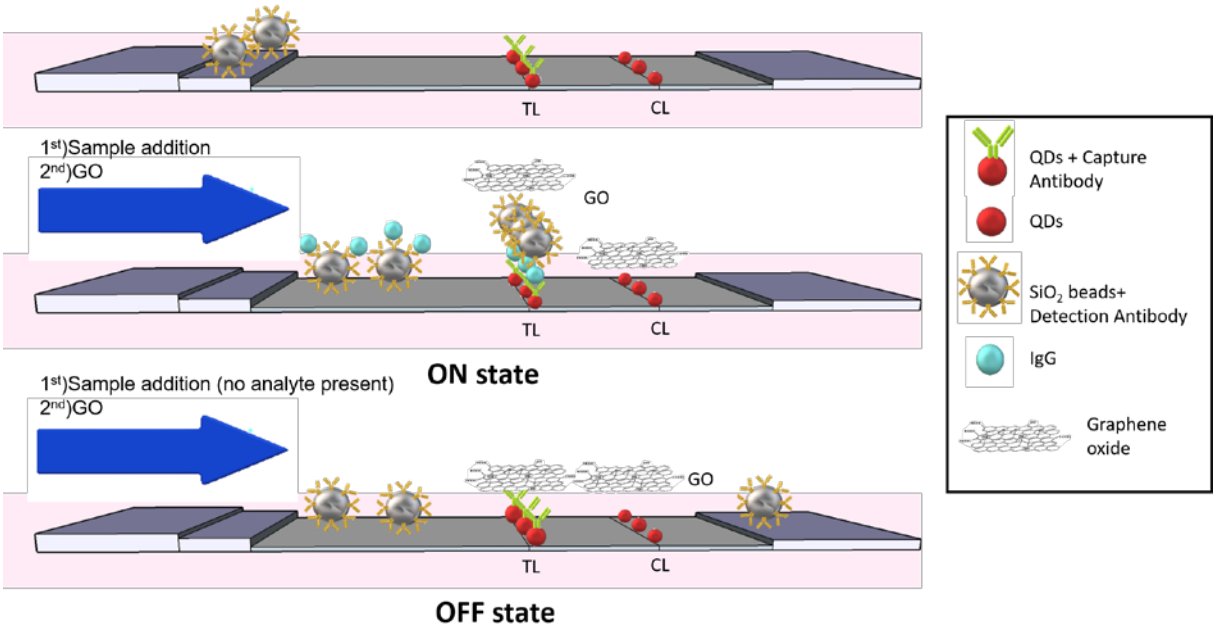

Figure 2. SEM micrographs of the lateral flow strip. Test line before adding GO (A) and after GO addition (B). Control line before adding GO (C) and after GO addition (D).

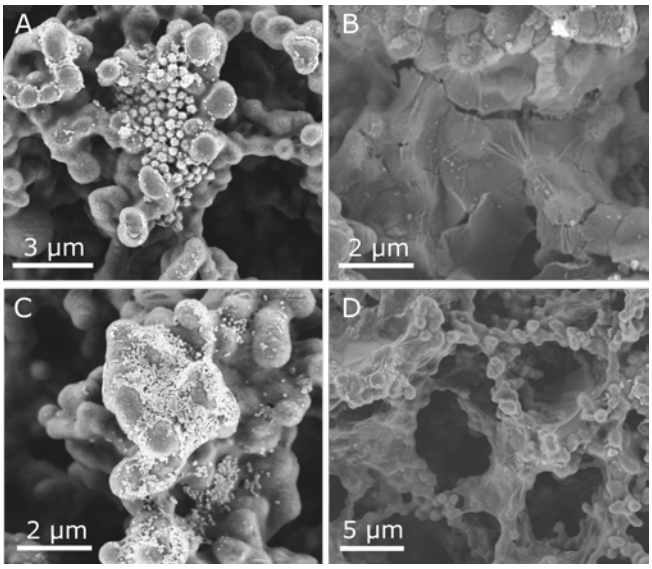

Figure 3. Representation of measurements in stardard buffer for test and control line of each concentration of IgG (a) , the bars represents % of quenching (coefficient of final intensity and initial), (b) normalized values (Q_{TL}/Q_{CL}) and (c) same experiment using monoclonal antibody, (d) normalized values.

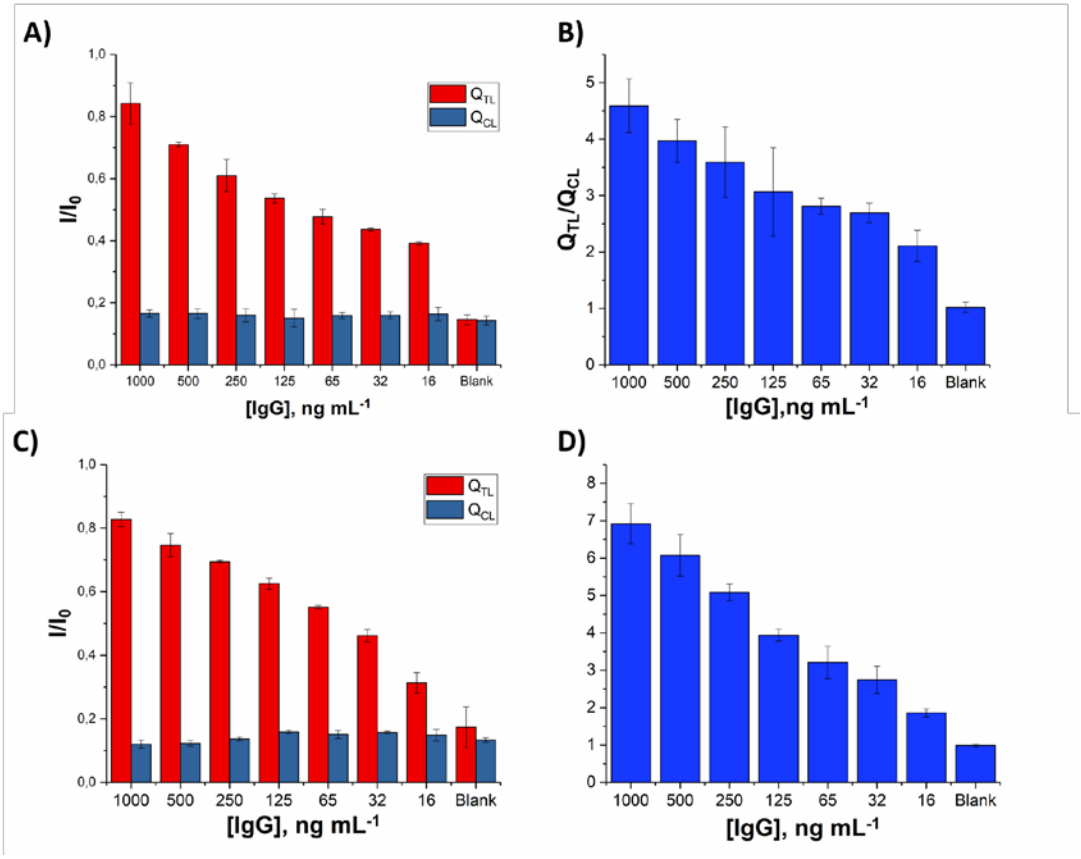

Figure 4. Results of measurements in human serum. (A) Comparison of T_L and C_L of each strip (B) normalized values

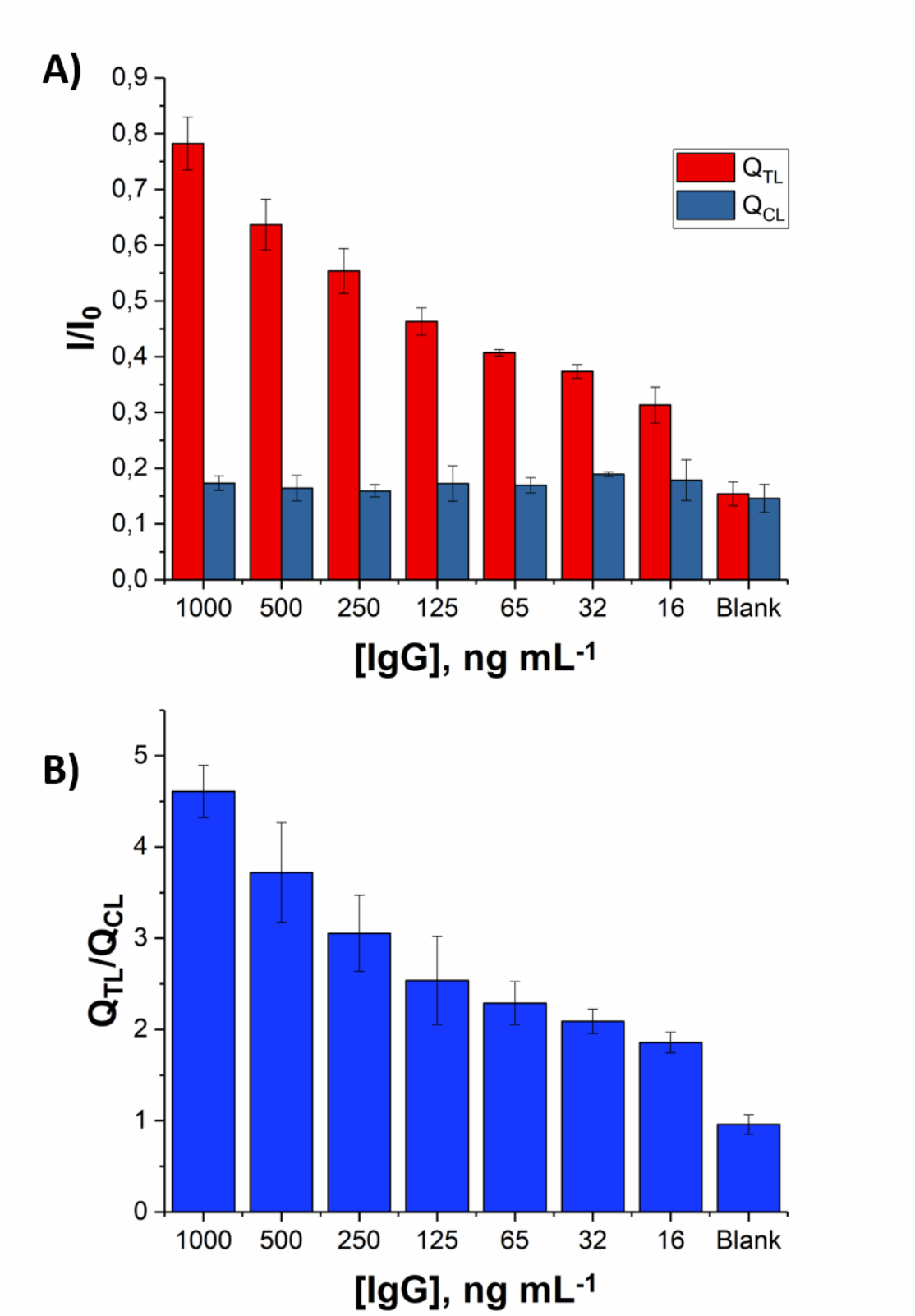

Table 1. Comparison of LOD for IgG detection.

LF strategy	Range	LOD	Technique	REF
Conventional LF	5-500 ng mL^{-1}	8-12 ng/mL	Colorimetric	Lab Chip, 2014,14, 4406-4414Lab Chip**,** 2015,15, 399-405
LF with wax pillars onto the detection pad	5-500 ng mL^{-1}	6,6 ng/mL	Colorimetric	Lab Chip, 2014,14, 4406-4414
gold nanoparticles loaded with enzymes	2-10 ng mL^{-1}	2 ng mL^{-1}	Colorimetric	Biosensors and Bioelectronics 40 (2013) 412–416
LF QDs-GO (this work)	1-20 ng mL^{-1}	1,35 ng mL^{-1}	Fluorescence	-

Supporting Information

Photoluminescent lateral flow based on non-radiative energy transfer for protein detection in human serum

Alejandro Zamora-Gálvez[a], *Eden Morales-Narváez*[a,b], *Javier Romero*[a], *and Arben Merkoçi*[a,c]*

[a] ICN2 Nanobioelectronics & Biosensors Group, Institut Català de Nanociència i Nanotecnologia, Campus UAB, Bellaterra, Barcelona 08193, Spain.

[b] Biophotonic Nanosensors Laboratory, Centro de Investigaciones en Óptica, A. C. Loma del Bosque 115, Colonia Lomas del Campestre, Leon 37150, Guanajuato, Mexico.

[c] ICREA Institució Catalana de Recerca i Estudis Avançats, Barcelona 08010, Spain

* arben.merkoci@icn2.cat

Figure S1. Optimization of QDs concentration.

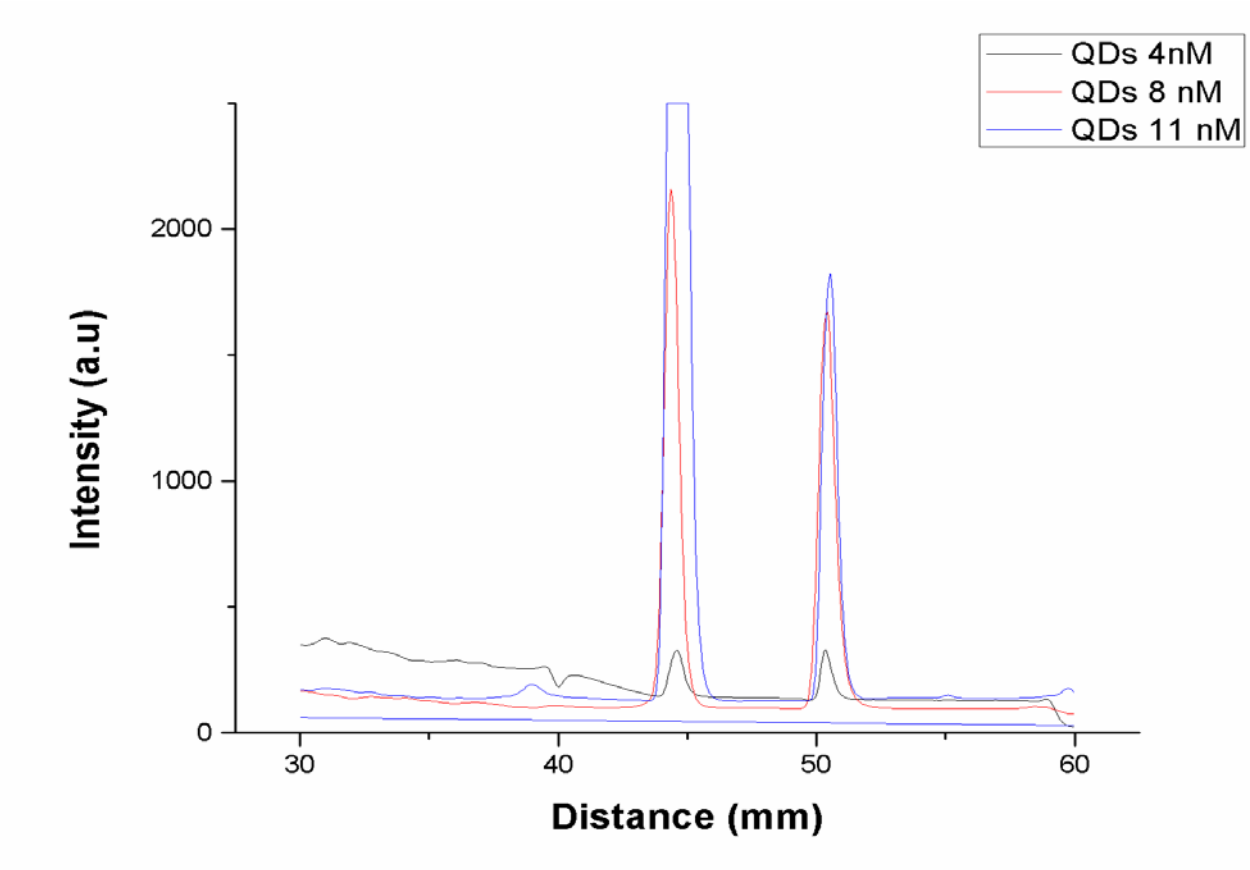

Figure S2. Optimization of graphene oxide concentration.

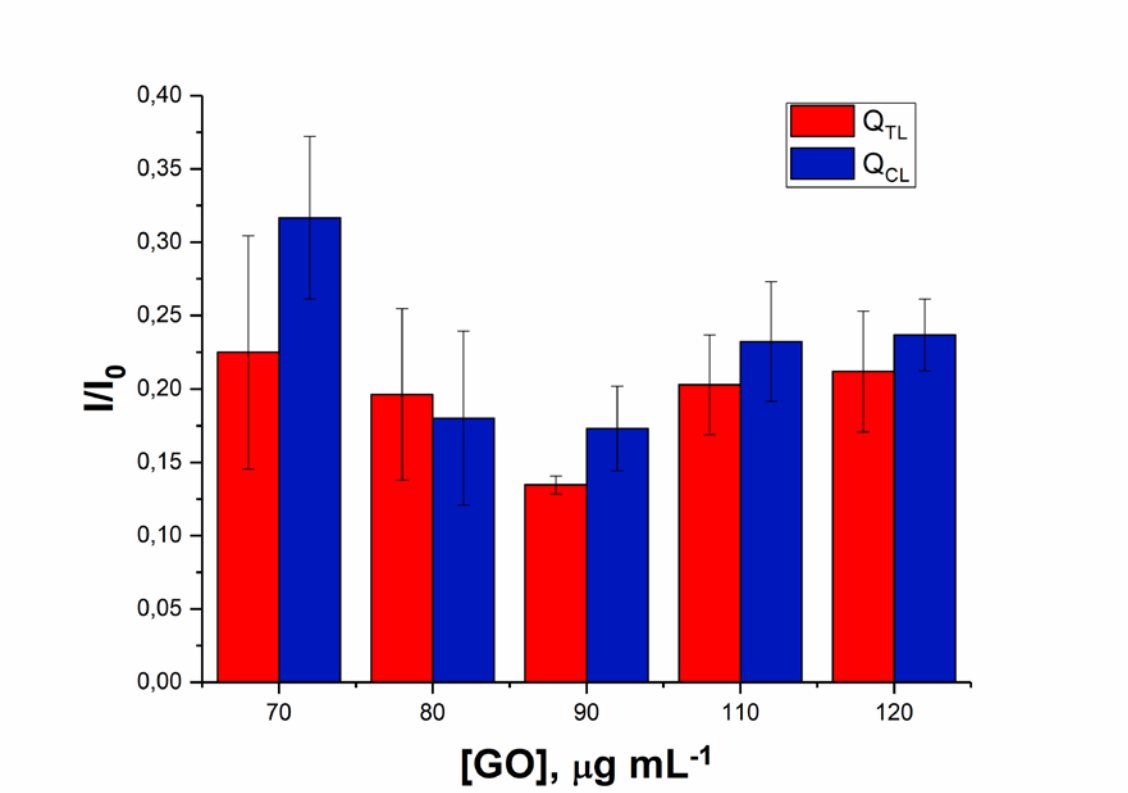

Figure S3. SEM micrographs of SiO_2 NPs of (A) 300nm and (B) 650 nm.

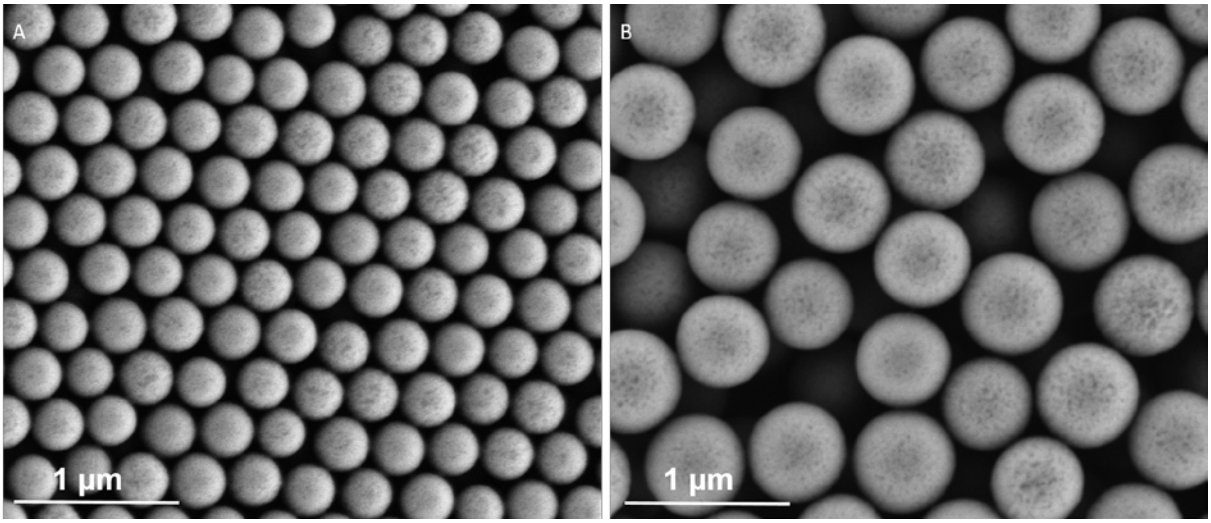

Figure S4. Optimization of SiO_2 NPs size, a) 300 nm, b) 650nm and c) comparative graphic

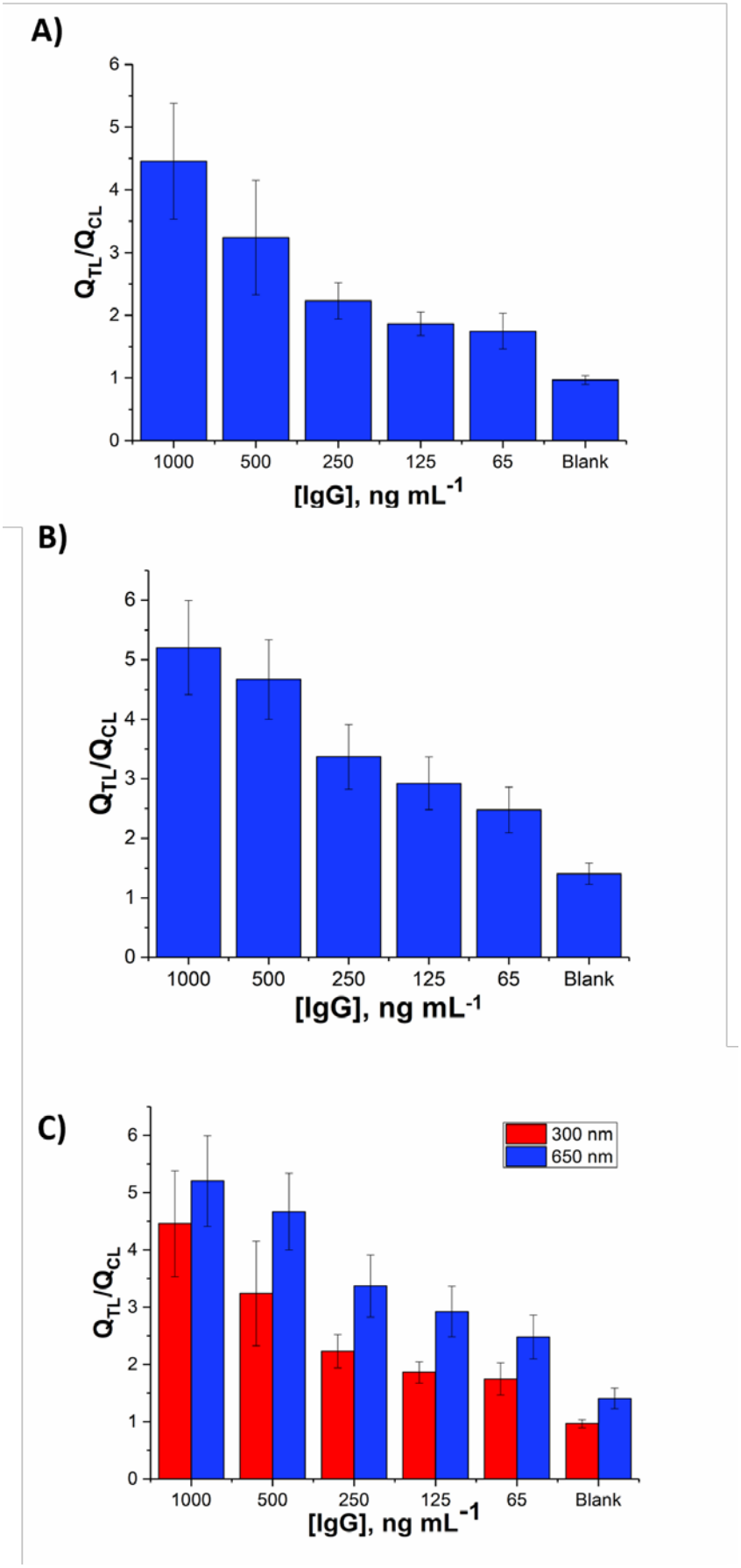

Figure S5. Profile of the photoluminescent intensity of the explored lateral flow strips at different concentrations of IgG.

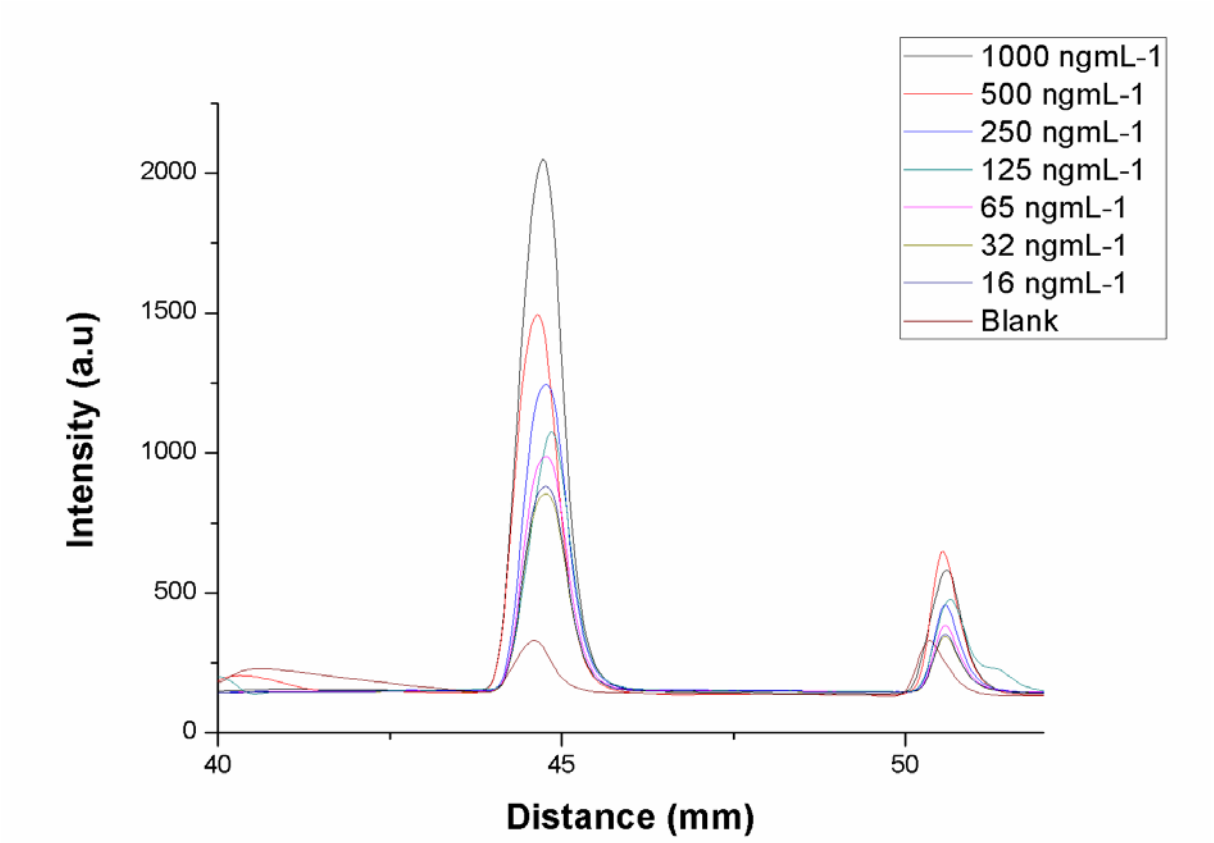

Figure S6. Calibration curve of IgG measurements with polyclonal (a) and monoclonal (b) antibody and in human serum (c).

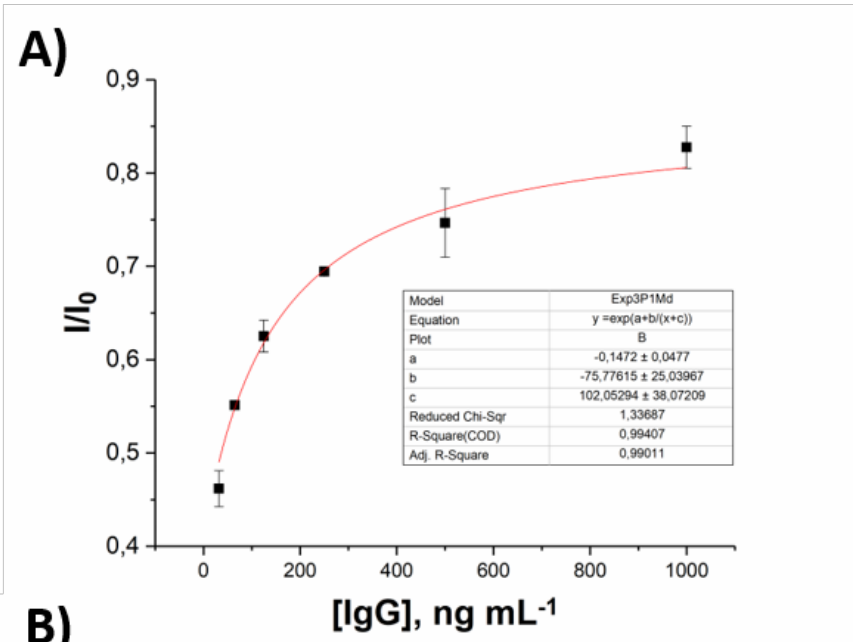
A)
I/I0
[IgG], ng mL-1
Model Exp3P1Md
Equation y =exp(a+b/(x+c))
Plot B
a -0,1472 ± 0,0477
b -75,77615 ± 25,03967
c 102,05294 ± 38,07209
Reduced Chi-Sqr 1,33687
R-Square(COD) 0,99407
Adj. R-Square 0,99011

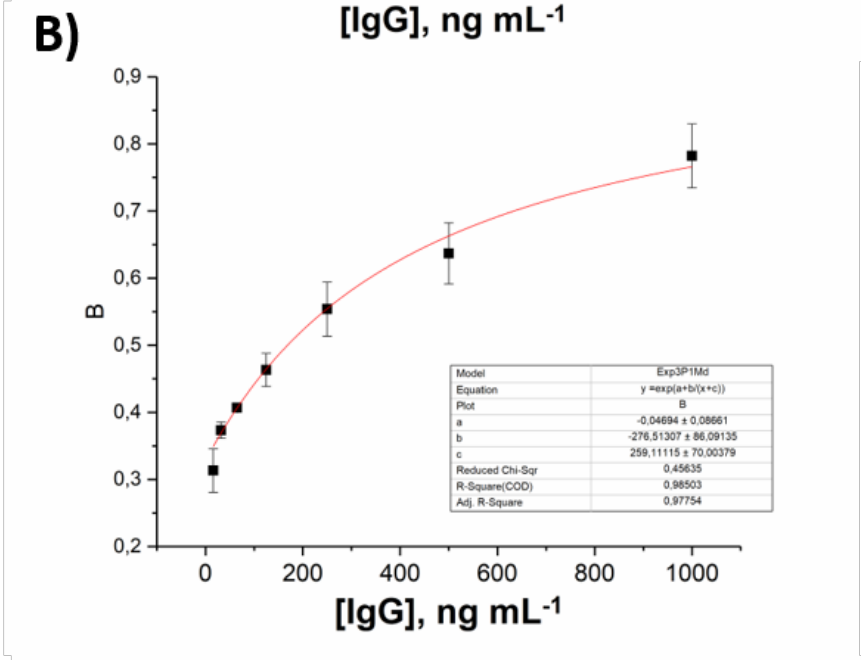
B)
B
[IgG], ng mL-1
Model Exp3P1Md
Equation y =exp(a+b/(x+c))
Plot B
a -0,04694 ± 0,08661
b -276,51307 ± 86,09135
c 259,11115 ± 70,00379
Reduced Chi-Sqr 0,45635
R-Square(COD) 0,98503
Adj. R-Square 0,97754

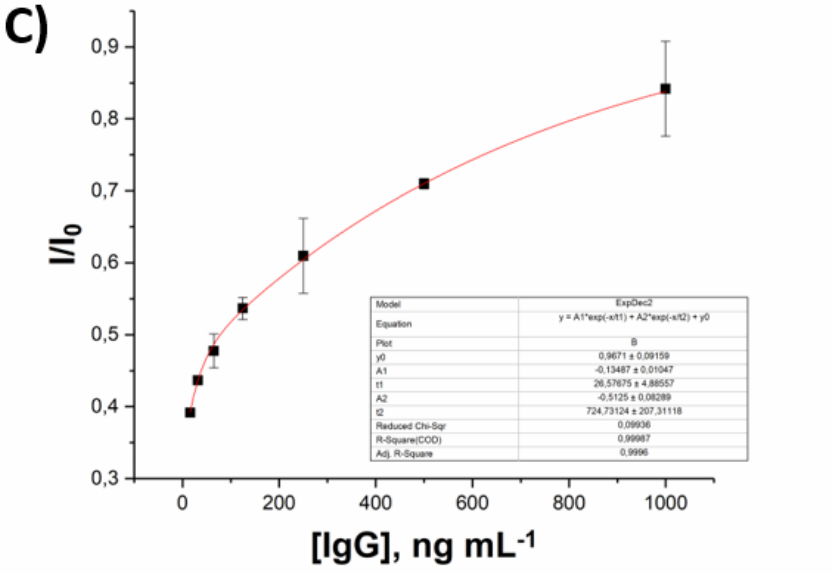
C)
I/I0
[IgG], ng mL-1
Model ExpDec2
Equation y = A1*exp(-x/t1) + A2*exp(-x/t2) + y0
Plot B
y0 0,9671 ± 0,09159
A1 -0,13487 ± 0,01047
t1 26,57675 ± 4,88557
A2 -0,5125 ± 0,08289
t2 724,73124 ± 207,31118
Reduced Chi-Sqr 0,09936
R-Square(COD) 0,99987
Adj. R-Square 0,9996